Asian J. Adv. Basic Sci.: **2017, 5***(1)*, 52-58
ISSN (Print): 2454 – 7492
ISSN (Online): 2347 – 4114
www.ajabs.org

Effect of Power Law Model on Cylindrical Surface Texture on the Isothermal Performance of Parallel Plates

Pankaj Kasib[1*], S. Kango[1], R. Jamwal[2], S. Vaibhav[2] & Ravi Kant Badhwa[2]

[1 & 2] School of Engineering & Technology, Career Point University, Hamirpur, INDIA
[*] Correspondance: E-mail: pankasib@gmail.com & s3kango@gmail.com

(Received 10 April, 2017; Accepted 26 April, 2017; Published 05 May, 2017)

ABSTRACT: The present study investigates the effect of cylindrical surface texturing obeying power law model on finite parallel plates. The modified Reynolds equation is solved numerically through finite difference approach with central differencing scheme. It has been observed that the combined effect of non Newtonian rheology and cylindrical surface textured improve the performance of parallel plates according to the operating parameters i.e. speed, load and dimple depth.

Keywords: Cylindrical surface textures; finite difference method; isothermal analysis; lubricant pressure; load; Power law model and Reynolds equation.

INTRODUCTION: Lubrication between two parallel sliding surfaces separated by a micro lubricant film thickness is of critical importance for precision machinery parts like mechanical seals. Micro-dimples or surface textures provide the lubrication effect between the two interfaces, if the interface operates under boundary and mixed regimes. In the textured surface, a sub atmospheric pressure is generated, when the lubricant passes through the land and reaches the inlet of dimple. It generates a pressure drop, which sucks the lubricant between the parallel plates, this increased lubricant flow enhances the pressure generation at the interface, which cause to generate the load carrying capacity in comparison to smooth parallel plates[1-3]. Brizmer et al.[4] theoretically investigated the effect of laser spherical surface texturing on the performance of parallel thrust bearing. Authors have been founded that the surface texturing has the form of micro dimples with preselected diameter, depth and area density. These authors adopted optimum parameters of the dimples, and best LST mode, to obtained maximum load carrying capacity for thrust bearing having parallel mating surfaces. Olver et al.[5] concluded that the maximum load carrying capacity occurs, when the pocket is located near the inlet to the bearing.

Meng et al.[6] investigated an effect of dimples on friction of parallel surfaces under different sliding conditions. Authors observed that the dimples can reduce the friction coefficient, when the film thickness to roughness ratio is small. Yu et al.[7] has been investigated the effect of different dimple shapes on the tribological performance of surface texturing. Authors concluded that a better friction reduction effect compared with untextured specimens can be obtained by selecting a suitable dimple area ratio and dimple depth for each dimple shape. Yuan et al.[8] investigated the orientation effect of micro-grooves on sliding surfaces. Authors observed that the grooves perpendicular or parallel to the sliding direction have a strong impact on the friction performance of sliding surfaces, and the merits of perpendicular or parallel orientation may swap under different contact conditions. Fesanghary et al.[9] using mathematical optimization methods for optimum periodic surface groove that provide the highest load carrying capacity(LCC) in parallel flat surface bearings are obtained. Authors found that optimally designed grooves can provide up to 36% more LCC compared to the conventional spiral grooves.

Malik & Kakoty[10] analyzed the effect of texturing on parallel and inclined slider bearing. Authors observed that the forward texturing has better performance than backward texturing. Uddin & Liu[11] has been optimized the geometric texture for the enhancement of hydrodynamic lubrication performance of parallel slider surfaces. Authors observed that the potential benefit of the proposed new shape enhancing the hydrodynamic lubrication performance of slider bearing contacts. Kasib et al.[12] investigated the isothermal analysis of the cylindrical textured hydrodynamic parallel plates. Authors found that the load carrying capacity of textured parallel plate increases with the increment of the number of textures in z direction. However, the fruitfulness of texturing deteriorated in the x-direction after certain point.

Recent days, the multi grades oils are used in mechanical machinery. These multi grades improved the viscosity index of the lubricant, which improves the performance of mechanical machinery. Based on the above literature review, it is noticed that surface texturing concept is very fruitful in the case of lubrication problems. However, in above literature, all the research has been done with Newtonian fluids. The Power law model can be used to describe the lubricant rheology easily and accurately. Both pseudo plastic and dilatant fluids (two important classes of non-Newtonian lubricants) can be characterized by the Power law model. Dien and Elrod[13] proposed the generalized Reynolds equation for analyzing the non-Newtonian effects in hydrodynamic bearings with Power law model. Various researchers[14-17] has been used this Power law model to investigate the non- Newtonian effects on slider and journal bearing. Huynh[15] concluded that the performance of bearings relates strongly to the extent and location of such limited corrugation as well as the non- Newtonian effect. Authors[16-17] observed that the load carrying capacity and friction force is increased with shear thickening fluids in both bearings (smooth and rough journal bearings). In above discussion, authors found that the research articles on the combined effect of surface texturing and Power law model on the performance of slider and journal bearing is available in open literature. However, authors did not find the research article for textured parallel plates along with Power law model. Thus, the objective of this paper is to present a numerical model for the isothermal analysis of hydrodynamically lubricated parallel plates having cylindrical surface dimpling on the bottom plate with Power law model.

MATHEMATICAL AND COMPUTATIONAL METHODS: The variation of pressure in y-direction is very small as compared to pressure in x and z directions respectively as the film thickness is in microns; the continuity and Navier stokes equations in Cartesian coordinates thus reduce to:

$$\frac{\partial u}{\partial x}+\frac{\partial w}{\partial z}=0 \tag{1}$$

$$\frac{\partial p}{\partial x}=\frac{\partial \tau_{yx}}{\partial y} \tag{2a}$$

$$\frac{\partial p}{\partial z}=\frac{\partial \tau_{yz}}{\partial y} \tag{2b}$$

$$\frac{\partial p}{\partial y}=0 \tag{2c}$$

$$\tau_{yx}=\eta\frac{\partial u}{\partial y} \tag{3a}$$

$$\tau_{yz}=\eta\frac{\partial w}{\partial y} \tag{3b}$$

where; u and w are the velocity component in x and z direction respectively, and η is the dynamic viscosity of the lubricant.

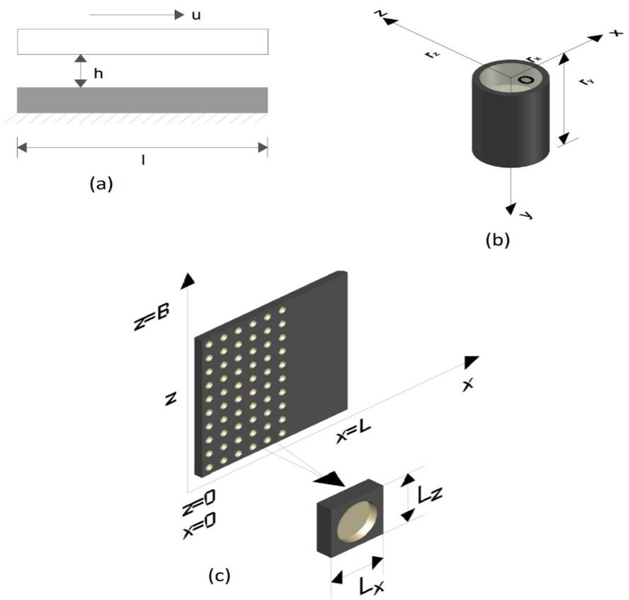

Figure 1: Schematic diagrams for (a) Smooth parallel plates (b) Cylindrical Surface texture details (c) Textured bottom plate.

The power model for lubricant viscosity is given by [Jang and Chang (1988)]:

$$\eta=m\left|\frac{\partial u}{\partial y}\right|^{n-1} \tag{4}$$

Where; m denotes the consistency index and n represents the flow behavior index. For $n = 1$, the lubricant is Newtonian, for $n < 1$, it is pseudo plastic (shear thinning) lubricant whereas, for $n > 1$, it characterizes dilatants lubricant (shear thickening). Equations (3a) and (3b) reduce to:

$$\tau_{yx}=m\left|\frac{\partial u}{\partial y}\right|^{n-1}\frac{\partial u}{\partial y}=m\left|\frac{\partial u}{\partial y}\right|^{n} \tag{5a}$$

$$\tau_{yz}=m\left|\frac{\partial u}{\partial y}\right|^{n-1}\frac{\partial w}{\partial y} \tag{5b}$$

Using equations (2a), (2b), (5a) and (5b), the new equation becomes:

$$\frac{\partial p}{\partial x}=m\frac{\partial}{\partial y}\left|\frac{\partial u}{\partial y}\right|^{n} \tag{6a}$$

$$\frac{\partial p}{\partial z}=m\frac{\partial}{\partial x}\left[\left|\frac{\partial u}{\partial y}\right|^{n-1}\frac{\partial w}{\partial y}\right] \tag{6b}$$

The boundary conditions at bearing surface are:

$y = 0$: $u = 0$; $y = h$: $u = U$ and $y = 0$: $w = 0$; $y = h$: $w = 0$ (7)

In present work, binomial expansion method is used to obtain the velocity component. In Binomial expansion higher terms are neglected for simplification.[16] Integration of equation (6a) with respect to y, and using binomial method while applying boundary conditions from equation (7), the velocity component in x-direction becomes:

$$u = \frac{Uy}{h} + \left|\frac{h}{U}\right|^{n-1}\left[\frac{\left(y^2 - yh\right)}{2mn}\frac{\partial p}{\partial x}\right] \tag{8a}$$

Similarly, equation (6b) is used to obtain velocity component in axial direction. To obtain the same the second term on right hand side of equation (8a) is neglected, to avoid complexity arises due to pressure gradients in x and z directions encountered while solving equation (6b).

$$u = \frac{Uy}{h} \tag{8b}$$

Differentiating equation (8b) with respect to y, we get:

$$\left|\frac{\partial u}{\partial y}\right| = \left|\frac{U}{h}\right|^{n-1} \tag{9}$$

Now equation (6b) reduces to:

$$\frac{\partial p}{\partial z} = m\frac{\partial}{\partial y}\left[\left|\frac{U}{h}\right|^{n-1}\frac{\partial w}{\partial y}\right] = m\left|\frac{U}{h}\right|^{n-1}\frac{\partial^2 w}{\partial y^2} \tag{10}$$

Using equation (10), the velocity component in z-direction is expressed as:

$$w = \left|\frac{h}{U}\right|^{n-1}\left[\frac{\left(y^2 - yh\right)}{2m}\frac{\partial p}{\partial z}\right] \tag{11}$$

Substituting velocity components from equations (8a) and (11) in equation (1) and integrating with respect to y, the non-Newtonian Reynolds-type equation for a parallel plate with power law fluid is obtained:

$$\frac{\partial}{\partial x}\left[\frac{h^{n+2}}{n}\frac{\partial p}{\partial x}\right] + \frac{\partial}{\partial z}\left[h^{n+2}\frac{\partial p}{\partial z}\right] = 6mU^n\frac{\partial h}{\partial x} \tag{12}$$

Where; p & h are the bearing pressure and nominal film thickness respectively whereas, m and U are notations for lubricant's viscosity and shaft speed respectively.

The lubricant film thickness in case of smooth parallel plate is written as:

$$h_{smooth} = C \tag{13}$$

In the proposed investigation, the cylindrical surface textures have been considered as shown in Fig. 1 (b). Three dimensional geometry and scheme of a cylindrical dimple is defined as follows [17]:

$$r_c = \sqrt{\left(x - x_c\right)^2 + \left(z - z_c\right)^2} \tag{14}$$

Where; r_c is the radius of cylinder

Dimple centre O_c (x_c, y_c, z_c) has been indicated in Fig. 1(c). The centre of the dimple is located on the surface of the bearing (i.e. $y_c = 0$). The expressions for x, x_c, and z_c are written as [14]:

$$x_c = n_1 a + \frac{(2n_1 - 1)}{2}L_x \quad \& \quad z_c = n_1 b + \frac{(2n_1 - 1)}{2}L_z$$

Where; L_x & L_z are the dimensions of unit cell & n_1 is number of dimples i.e. 1, 2, 3……..so on.

Expression for film thickness (h) in the computational domain is expressed as:

$$\begin{aligned} h &= h_{smooth} && \text{if} \quad r \geq r_c \\ &= h_{smooth} + r_y && \text{if} \quad r < r_c \end{aligned} \tag{15}$$

The pressure field in the lubricant film is numerically computed through equation (12) using finite difference method (FDM) with central differencing scheme. The pressure is computed iteratively through Gauss-Seidal method and an over relaxation factor of 1.7 is used for finding the solutions. The convergence criterion for Reynolds equation (3) is given below for pressure:

$$\frac{\sum\sum\left|\left(p_{i,k}\right)_l - \left(p_{i,k}\right)_{l-1}\right|}{\sum\sum\left|\left(p_{i,k}\right)_l\right|} < 10^{-07} \tag{16}$$

Where, i, k represent the number of nodes in x and z direction respectably and I is the number of Iterations.

The performance parameters viz. the load carrying capacity (W), the friction force and (F), and friction coefficient (f) are calculated for parallel plate.

Load carrying capacity is calculated from the integration of pressure parallel to the x-axis and z-axis as:

$$\text{Load } (W) = \int_0^B\int_0^L p(i,k)\,dxdy \tag{17}$$

$$\text{Friction force } (F) = \int_0^B\int_0^L \left|\tau_{yx}\right|_{y=0} dxdy \tag{18}$$

$$\text{Where} \quad \tau_{yx} = m\left[\frac{\partial u}{\partial y}\right]^n \tag{19}$$

Coefficient of friction (f) = $\dfrac{F}{W}$ (20)

Load carrying capacity and friction force are obtained numerically through double integration by Simpson's 1/3rd rule.

RESULTS AND DISCUSSION: The input data for parallel plates attributes of textures and operational parameters employed in this work are presented in table 1 and some of the data has been taken from published experimental paper [Shen and Khonsari (2016)].

Table 1: Input data.

Sr. No.	Input parameters	Value
1.	Length of the plates(L)	0.1413m
2.	Width of the plates(B)	0.1413m
3.	Dynamic viscosity(η)	0.0064 Pa.s
4.	Viscosity consistency(m)	0.0064 Pa.s^n
5.	Speed(N)	100 & 1000 rpm
6.	Number of nodes in x-direction(N_x)	150
7.	Number of nodes in z-direction(N_z)	150
8.	Number of textures in x-direction (Nt_x)	6
9.	Number of textures in z-direction (Nt_z)	10
10.	Dimple depth (r_y)	1-7µm
11.	Dimple radius (r_c)	0.004m
12.	Length along x-direction (L_x)	0.008m
13.	Length along z-direction (L_z)	0.008m
14.	Distance between two successive unit cells in x-direction (a)	0.0055m
15.	Distance between two successive unit cells in z-direction (b)	0.0055m
16.	Clearance(C)	10µm

The input data are also provided along with figures being presented. Kasib et al.[12] has been investigated the effect of number of cylindrical textured on the performance of parallel plates for Newtonian lubricants & observed that the 6 number of textures in x-direction increase the load carrying capacity of the parallel plates. Beyond this, the fruitfulness of texturing deteriorated. Therefore, in present investigation, authors used 6 numbers of textures for further study. 3-Dimensional representations of lubricating film thickness are shown in Fig 2 (a) & (b) for smooth and cylindrical textured plate respectively.

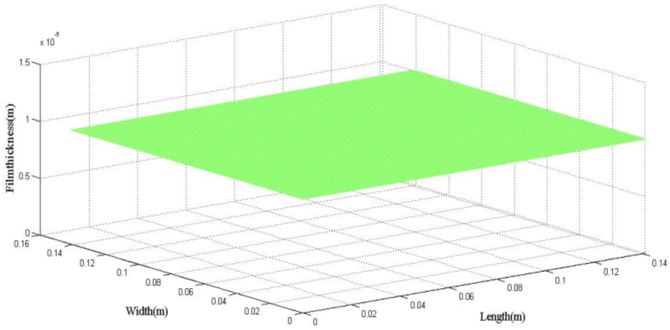

(a) $Nt_x = 0$ & $Nt_z = 0$

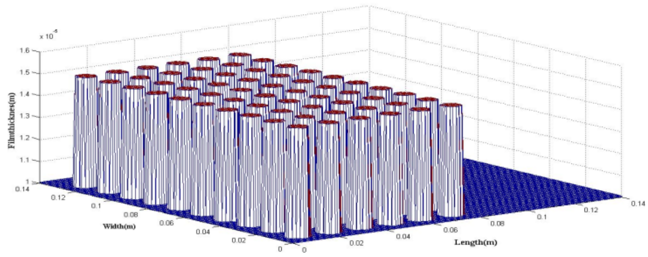

(b) $Nt_x = 6$ & $Nt_z = 10$

Figure 2: Dimensional representation of lubricant film thickness (a) Smooth Plate (b) Texture Plate.

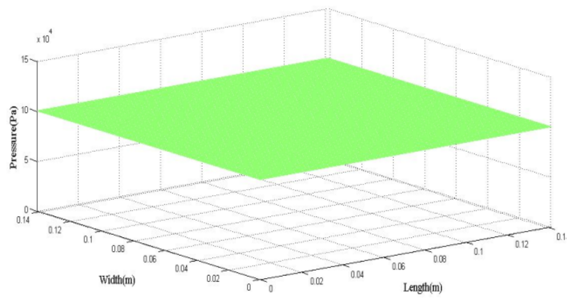

(a) $Nt_x = 0$ & $Nt_z = 0$

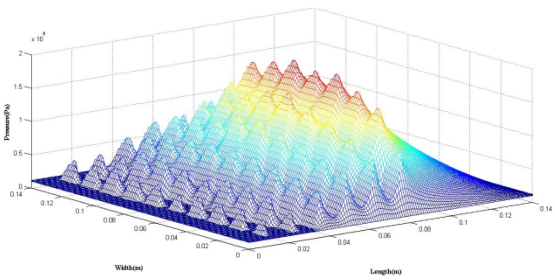

(b) $Nt_x = 6$ & $Nt_z = 10$

Figure 3: Dimensional representation of lubricant pressure (a) Smooth Plate (b) Texture Plate.

Fig 3 (a) shows that there is no generation of lubricant pressures in the case of smooth plate. However, there is the generation of lubricant pressures between the smooth & textured surface as shown in Fig 3 (b).

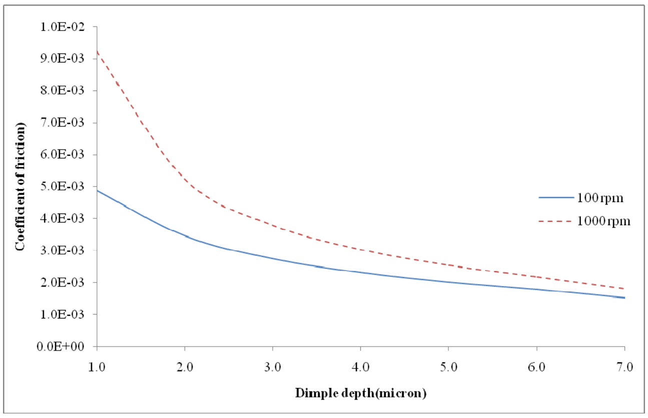

Figure 4: Effect of dimple depth on coefficient of friction for different speed [m=0.0064 Pa.s^n, C=10µm, n=1, Nt_x=6, Nt_z=10].

The combined effect of different speeds and dimple depth are presented in Fig.4. It has been observed that at low dimple depths the slope of the reduction of coefficient of friction is more as shown in fig 4 for both the speeds. However, at high dimple depths, the reduction is almost constant. The gap between two profiles at low & high speed is also very less as compared with the gap at low dimple depth.

It has been seen that the load carrying capacity increases with slow rate up to n=1 & after that it is very high for n=1.1 as shown in fig 5 for both the speeds. It may be happened due to the high viscosity in the case of shear thickening fluids.

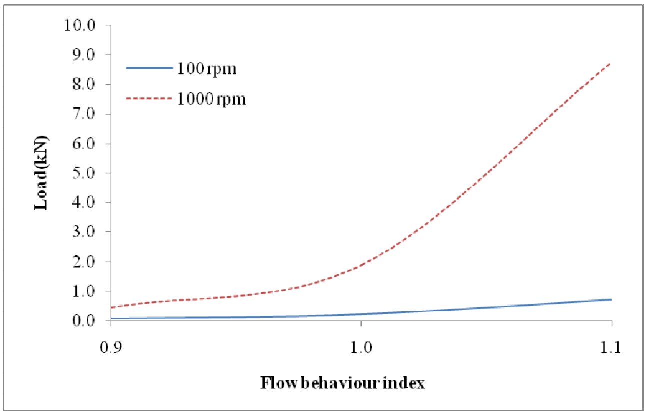

Figure 5: Variation of load w.r.t flow behaviour index at different speed [m=0.0064 Pa.s^n, C=10µm, Nt_x=6, Nt_z=10].

Combined effect of dimple depth, flow behaviour index & speed on the performance of parallel plates are presented in fig. 6. It has been observed that more reduction in coefficient of friction is achieved for shear thinning fluid at low speed. However, the coefficients of friction are almost same in the case of Newtonian and shear thickening fluids. At high speed, the shear thickening fluids show more reduction as compared with rest of two lubricants.

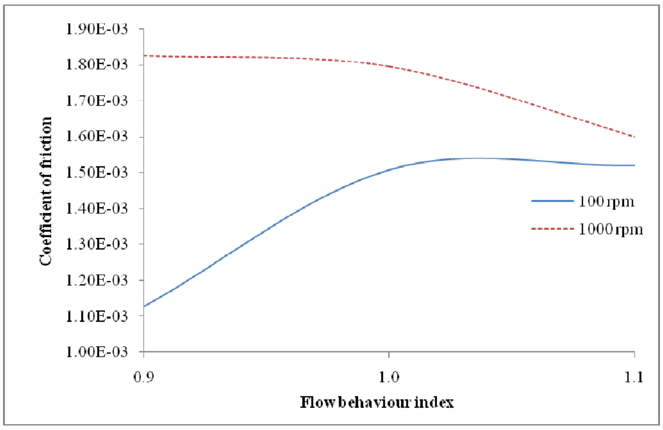

Figure 6: Variation of coefficient of friction w.r.t flow behaviour index at different speed [m=0.0064 Pa.s^n, C=10µm, Nt_x=6, Nt_z=10].

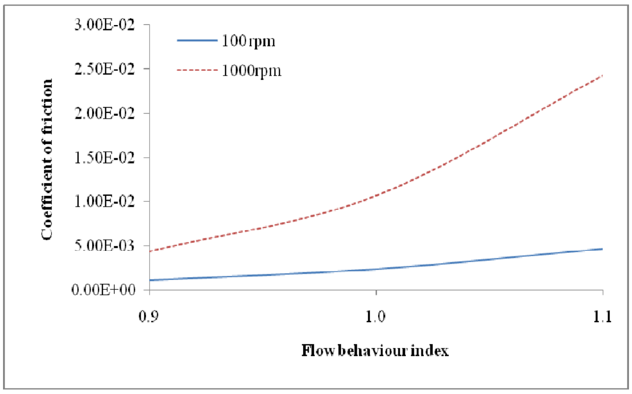

Figure 7: Effect of speed on coefficient of friction for different flow behaviour index at constant load [W=100N, r_y=7 micron, m=0.0064 Pa.s^n, Nt_x=6, Nt_z=10].

In figs. 4 to 6, authors calculated the performance parameters at constant clearance (10 µm). However, in figs. 7 to 9, the clearances between the plates are varying by keeping the load constant.

Combined effect of coefficient of friction, flow behaviour index & speed are presented in fig 7. It has been observed that more reduction in coefficient of friction is achieved for shear thinning fluid, then Newtonian and then shear thickening fluid for high and low speed.

It has been depicted from fig. 8 that shear thickening fluids show maximum clearance between two parallel plates for both the speeds. As the generated lubricant pressures are very high in this case, this caused to high coefficient of friction in these fluids as shown in fig. 7. However, the shear thinning fluids show less clearance and less lubricant pressures are generated as compared with Newtonian and shear thickening fluids, which cause to less frictional coefficient for textured parallel plate.

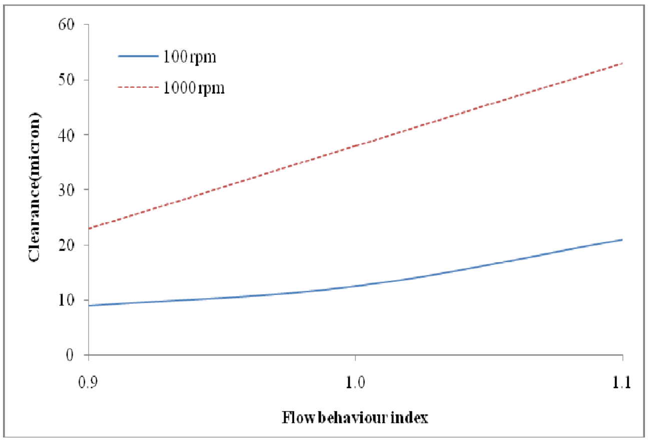

Figure 8: Effect of speed on clearance for different flow behaviour index at constant load [W=100N, r_y=7 micron, Nt_x=6, Nt_z=10].

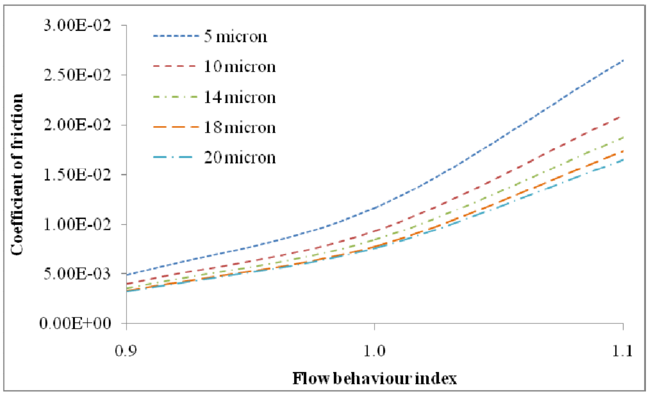

Figure 9: Effect of speed on clearance for different flow behaviour index at constant load [W=100N, U=1000rpm, Nt_x=6, Nt_z=10].

Fig. 9 shows the effect of dimple depth and flow behaviour index on the friction coefficient performance of textured parallel plate at high speed. It has been observed that by increasing the dimple depth the coefficient of friction reduces for all types of lubricants. However, at high dimple depth the performance is almost constant.

CONCLUSION: The influence of cylindrical textures along with lubricant rheology has been investigated for parallel plates. Following are the broad outcomes of present study:

1. Shear thinning fluids (n=0.9) improves performance of textured parallel plate at low speed. However, the more reduction in coefficient of friction is achieved at high speed for shear thickening fluids (n=1.1)

2. Shear thinning fluids has less coefficient of friction as compared with Newtonian and shear thickening fluids at constant load.

3. More reduction in coefficient of friction is achieved for deep dimples.

ACKNOWLEDGEMENT: The authors thank the Career Point University for providing the infrastructure and lab facilities. The State Council for Science, Technology & Environment, Himachal Pradesh is highly acknowledged for its technical and human support.

REFERENCES:

1. Etsion I. (2005) State of art in laser surface texturing, *Journal of Tribology*, 27, 248-253, 0742-4787.
2. Etsion I. (2013) Modeling of surface texturing in hydrodynamic lubrication, *Friction*, Volume 1(3), 195-209, 2223-7690.
3. Gropper D., Wang L. and Harvey T.J. (2016) Hydrodynamic lubrication of textured Surfaces: A review of modeling, *Tribology International*, 94, PP. 509-529, ISSN 0301-679X.
4. Brizmer V., Kligerman Y. and Etsion I. (2003) A Laser Surface Textured Parallel Thrust Bearing, *Tribology transactions, 46*, 397-403.
5. Olver A.V., Fowell M.T., Spikes H.A. and Pegg I.G. (2006) Inlet suction', a load support mechanism in non-convergent, pocketed, hydrodynamic bearing, J. *Engineering tribology, 220*, 105-108.
6. Meng F., zhou R., Davis T., Cao J., Wanga Q.J., Hua D. and Liu J. (2010) Study on the effect of dimples on friction of parallel surfaces under different sliding conditions, *Applied surface science, 256*, 2863-2875.
7. Yu H., Deng H., Huang W. and Wang X. (2011) The effect of dimple shapes on friction of parallel surfaces, *J. Engineering tribology, 225*, 693-703.
8. Yuan S., Huang W. and Wang X. (2011) Orientation effects of micro-grooves on sliding surfaces, *Tribology international, Volume 44*, 1047-1054.
9. Fesanghary M. and Khonsari M.M. (2013) On the optimum groove shapes for load-carrying capacity enhancement in parallel flat surface bearings: Theory and experiment, Tribology *international, 67*, 254-262.
10. Malik S. and Kakoty S.K. (2014) Analysis of dimple textured parallel and inclined slider bearing" *journal of engineering, Volume 228*, 1343-1357.
11. Uddin M.S. and Liu Y.W.(2016) Design and optimization of a new geometric texture shape for the enhancement of hydrodynamic lubrication performance of parallel slider surfaces, *Biosurface and Biotribology, Volume 2*, 59-69.
12. Kasib P., Kango S., Jamwal, R., and Vaibhav S. (2017) Isothermal analysis of the cylindrical textured hydrodynamic parallel plates, *National conference on Advances in Basic & Applied Sciences during April 07-08, 2017 at Career Point University, Hamirpur (HP).*

13. Dien I.K. and Elrod H.G. (1983) A generalized steady-state Reynolds equation for non-Newtonian fluids, with application to journal bearings, ASME Journal of Lubrication Technology, 105, 385-390.

14. Jang J.Y. and Chang C.C (1988) Adiabatic analysis of finite width journal bearings with non-Newtonian lubricants, *Wear*, Vol. 122, 63-75.

15. Huynh B. P. (2011) Numerical investigation of slider bearings with limited corrugation and power law lubricant, *Proceedings of the ASME, IMECE2011-65272.*

16. Kango S. and Sharma RK. (2010) Studies on the influence of surface texture on the performance of hydrodynamic journal bearing using power law model, *Int. J. Surface Science and Engineering*, *4*, 505-524.

17. Kango S. Sharma R.K. Pandey R.K. (2014) Thermal analysis of microtextured journal bearing using non-Newtonian rheology of lubricant and JFO boundary conditions, *Tribology International*, 69, 19-29.

18. Shen C. and Khonsari M.M.(2016) Texture Shape Optimization for Seal-like Parallel Surfaces: Theory and Experiment, *Tribology Transactions*, 1-32, 1547-397X.